

In vivo measurements of ocular accommodation

E. Frederick^{1,2}, K. Richdale³, M. Hrovat⁴, and S. Patz²

¹Physics, UMass Lowell, Lowell, 883 Broadway St, United States, ²Radiology, Brigham and Women's Hospital, Boston, MA, United States, ³College of Optometry, Ohio State University, Columbus, OH, United States, ⁴Mirtech Inc, Brockton, MA, United States

Introduction

Presbyopia is the only ocular condition that affects all individuals over the age of 50; regardless of race or gender [1]. The Helmholtz theory for presbyopia postulated that the lens loses its ability to change shape and thus cannot focus on near objects due to sclerosis. Helmholtz's theory has been challenged by more recent research that suggests that changes in the ciliary body, zonules, and/or arrangement of the structures of the accommodative system lead to accommodative decline [2,3]. In fact, it has been demonstrated that all of the accommodative structures change either their structure or function with age [1,2,3,4]. In light of these results, and the fact that no one mechanism for the development of presbyopia can account for the early onset and complete loss of accommodation, it seems logical that presbyopia may be the additive result of multiple changes in the accommodative system.

MRI is an excellent modality to monitor changes in the accommodative structures of the eye as it is the only technique that allows for *in vivo* imaging of the entire globe. However, due to the small size of the orbit, blinking and eye saccades, ocular imaging is technically difficult. Previous reports demonstrate the clinical usefulness of MRI, but are limited by poor spatial resolution, long imaging times, and motion artifacts [5,6,7]. Recently, Bert *et al.* were able to minimize the motion artifacts related to blinking by taping one of the eyes shut and allowing the contralateral eye to focus on a target [8]. For these experiments, we investigated the accommodative changes in the eye due to focusing of the contralateral eye on distance and on near accommodative stimuli using the protocol developed by Bert *et al.* [8]

Methods

High-resolution MR images were acquired on two young, healthy, volunteers (male and female) with a 1.5T GE Signa system (GE Medical Systems Waukesha, WI). A standard 2D multi-slice single spin echo pulse sequence was used: FOV=6cm, matrix 256x160, TE/TR =10/1400ms, 4 slices and slice thickness =2 and 3mm. The in-plane resolution was 234 μ m and total scan time was 112s. T₁ and T₂ for optimal contrast were obtained from Patz, *et al.* [9]. A custom 1"-diam surface coil was constructed and used for these experiments. The coil was taped over the left eye while the contralateral eye focused on a target. Because accommodation and tracking between the eyes are yoked [10], the right eye was used to fixate the target and the left eye was imaged to reduce the motion artifacts associated with blinking and eye saccades. Two charts were used as targets; a near chart located directly above the volunteer (22cm); and a distant chart presented at optical infinity using a mirror system. The subject fixated on a letter on distant chart or the smallest viewable line of the near chart. For all images, four chords were drawn over the length of the ROI and the mean chord length was computed for the region (Fig. 1).

Results

Excellent SNR was achieved with the custom RF coil, i.e. SNR of 36/19 was achieved in the ciliary body/lens nucleus. Table 1 shows the average ciliary body ring diameters, lens thicknesses, and lens diameters for the male (NWM) and female (NWF) subjects focusing on distant and near accommodative stimuli. Figure 2 presents side-by-side comparison of near vs. far accommodation. Note that the eyes are slightly rotated due to the small angular differences in the positions of the accommodative stimuli. As expected from prior studies [4,11], both the lens and ciliary body diameter decrease with increasing accommodation while the opposite is observed for the lens thickness.

Discussion

Our measurements of the lens dimensions agree with those reported by Strenk *et al.* [4,10], but our measurements of ciliary body diameter are ~2 mm smaller. This discrepancy may be due to individual variation, or a difference in how the measurements were made. Our results demonstrate the feasibility of using the contralateral eye to fixate and focus on an accommodative target while imaging the taped eye. This method virtually eliminates blinking in the imaged eye, which otherwise would be a major source of motion artifacts. Any remaining motion artifacts may be attributed to normal eye saccades. The ability to fixate on a target can be tiring and therefore minimization of the scan time is important. With our protocol, the scan time is half that of Strenk *et al.* [9,10].

References

1. Atchison, D. A. (1995). *Ophthalmic Physiol Opt* 15(4): 255-72.
2. Davanger, M. (1975). *Acta Ophthalmol (Copenh)* 53(1): 19-33.
3. Farnsworth, P. N. and S. E. Shyne (1979). *Exp Eye Res* 28(3): 291-7.
4. Strenk, S. A., L. M. Strenk, et al. (2006). *J Cataract Refract Surg* 32(11): 1792-8.
5. Atlas SW, Grossman RI, Savino PJ, et al. *AJNR Am J Neuroradiol* 1987;8:141-146.
6. Prummel MF, Gerding N, Zonneveld FW, Wiersinga WN. *Clin Endocrinol (Oxf)* 2001;54:205-209.
7. Simon EM, McCaffery S, Rowley HA, Fischbein NJ, Shimikawa A, O'Brien JM. *Neuroradiology* 2003;45:489-492.
8. Bert RJ, Patz S, Ossiani M, et al. *Acad Radiol* 2006;12:368-378.
9. Patz S, Bert RJ, Frederick E, Freddo TF. *J Magn Reson Imaging*. 2007 Sep;26(3):510-8.
10. Campbell, F. W. (1960). *J Opt Soc Am* 50: 738
11. Strenk, S. A., J. L. Semmlow, et al. (1999). *Invest Ophthalmol Vis Sci* 40(6): 1162-9.

Acknowledgements

This work was supported by NIH EY13825 and NIH EY 013359.

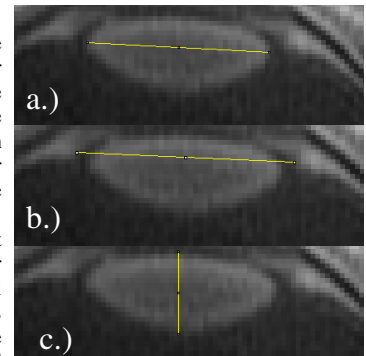


Figure 1. Four measurement were made and averaged for each region to determine the mean a.) equatorial lens diameter, b.) ciliary body's ring diameter, and c.) lens thickness.

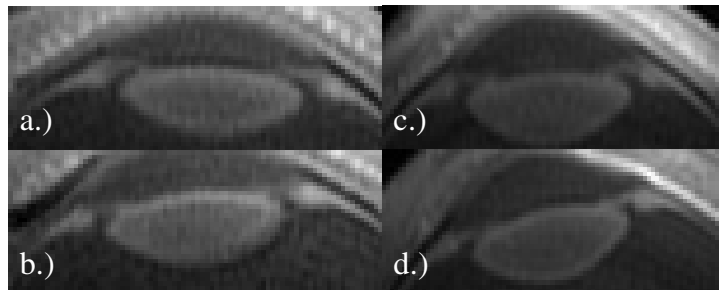


Figure 2. a & c: Subjects focused on the nearest target. b & d: Subjects focused on the farthest target.

Subject	ROI	Far	Near	Subject	ROI	Far	Near
		Mean \pm SD	Mean \pm SD			Mean \pm SD	Mean \pm SD
1	Ciliary Body	10.4 \pm 0.08	9.93 \pm 0.12	2	Ciliary Body	10.9 \pm 0.08	10.5 \pm 0.12
		9.38 \pm 0.17	8.71 \pm 0.20			9.73 \pm 0	9.17 \pm 0.12
	Lens	3.84 \pm 0.04	3.96 \pm 0.21		Lens	4.04 \pm 0	4.07 \pm 0.04

Table 1. The average chords lengths for each of the regions. Computed by averaging chord length of the region from two separate images: a 2mm and a 3mm thick image.